

## APPLICATION OF COMPUTATIONAL FLUID DYNAMICS MODELLING ON THE GRATE-KILN PROCESS AT LKAB

**Ulf SJÖSTRÖM<sup>1</sup>, Magnus LUNDQVIST<sup>1</sup> and Ola ERIKSSON<sup>2</sup>**

<sup>1</sup> MEFOS – Metallurgical Research Institute AB, PO Box 812, SE-971 25 Luleå, SWEDEN

<sup>2</sup> LKAB – Loussavaara Kiirunavaara AB, SE-981 86 Kiruna, SWEDEN

### ABSTRACT

Loussavaara Kiirunavaara AB (LKAB) supplies customized iron ore products for blast furnaces and direct reduction processes. The products are mainly pellets, and today LKAB operates five pelletizing plants located in Malmberget and Kiruna, Sweden.

A research programme together with MEFOS was initiated during 2005 to meet future demands for lower emissions and to improve the process efficiency in general. Computational Fluid Dynamics (CFD) has been chosen as a tool for the development due to the characteristics of the pellet induration process.

A heat transfer model for a porous bed applied on cooling of pellets for the Grate-Kiln process is described and another example focusing on combustion in kiln is briefly mentioned in the paper. The developed porous bed model is the base for further development in order to get accurate description of drying, preheating and oxidation of magnetite within a pellet during the production process. The aim is to develop a process model which can describe the complete time-temperature history from the first drying zone to the annular cooler. The model is intended to be used for studies of plant modifications and changed process gas flows on the production, energy consumption and pellet quality.

### NOMENCLATURE

$A_p$	surface area of pellet [m <sup>2</sup> ]
$A_f$	cell face area [m <sup>2</sup> ]
$d_p$	diameter of pellet [m]
$Nu$	Nusselt number defined by Eq.(4) [-]
$L_c$	average free radiation length [m]
$P$	pressure [Pa]
$Q_{conv}$	energy transport by convection [J]
$Q_{cond_b}$	energy transport by conduction in bed [J]
$Q_{cond_p}$	energy transport by conduction in pellet [J]
$Q_{rad}$	energy transport by radiation [J]
$r$	radius [m]
$Re_b$	Reynolds number for bed, $Re_b = \frac{\rho(\phi d_p)U}{\mu(1-\varepsilon)}$
$T_{surf}$	temperature at pellet surface [K]
$T_{gas}$	temperature in gas [K]
$\Delta t$	time step [s]
$U$	superficial velocity vector [m/s]
$x$	distance [m]

$\alpha_b$	heat transfer coefficient to bed [W m <sup>-2</sup> K <sup>-1</sup> ]
$\varepsilon$	porosity [-]
$\varepsilon_{rad}$	emissivity of pellet surface [-]
$\lambda_{gas}$	heat conduction in gas [W m <sup>-1</sup> K <sup>-1</sup> ]
$\lambda_p$	heat conduction in pellet [W m <sup>-1</sup> K <sup>-1</sup> ]
$\lambda_b$	heat conduction in bed [W m <sup>-1</sup> K <sup>-1</sup> ]
$\mu$	laminar dynamic viscosity [kg m <sup>-1</sup> s <sup>-1</sup> ]
$\rho$	density [kg m <sup>-3</sup> ]
$\sigma$	Stefan-Bolzmann constant [W m <sup>-2</sup> K <sup>-4</sup> ]
$\phi$	shape factor [-]

### Indexes

$i$	index for coordinate directions
$j$	index for neighbour cells
$k$	index for layers in a pellet

## INTRODUCTION

### Description of Grate-Kiln Process

LKAB has three pelletizing plants based on the Grate-Kiln process and a fourth plant, KK4, is under construction. The process consists of three parts; grate furnace with moving grate band, rotary kiln and an annular cooler, see flowsheet in Figure 1.

Wet green pellet balls are fed on the moving grate to form a bed depth of 0.20-0.25 m. The width varies between 4.6 and 5.66 m depending on plant. Slurry of ground iron ore rich in magnetite is the main raw material for balling operation to green pellet balls. Minerals like bentonite, olivine, quartz, lime and dolomite are also added depending on what pellet quality to be produced.

The grate furnace is more than 50 m long and includes four zones; Up-Draft-Drying (UDD), Down-Draft-Drying (DDD), Tempered-Pre-Heat (TPH) and Pre-Heat (PH). When the bed moves through the zones, process gas flows in cross flow through the bed. The pellets are dried, oxidized and preheated. A thermal gradient through the bed is developed with the top layer warmer than the bottom layer in contact with the moving grate. Except for heating by convection a very important thermal aspect is the chemical energy generated by the oxidation from magnetite to hematite.

Temperature is further increased in the rotary kiln by combustion where a single burner is located at the end of the kiln. Coal is combusted with preheated air in excess. The air comes from the first zone of the annular cooler, C1, and is preheated to approximately 1150°C. All modes

of heat transfer are active in the kiln but radiation from the hot flame and the kiln wall is dominating. The kiln is more than 30 m long and has an inside diameter of approximately 5 m. In the kiln the pellets are well mixed due to the rotation of the kiln and reaching a maximum temperature of 1280°C. The heat treatment gives strength to the pellets due to sintering. Normally, coal is used as fuel but oil is used as back up fuel during transient operation.

After the kiln the pellets are charged into the annular cooler and a fixed bed with a height of approximately 0.7 m is formed. Pellets are cooled down in four zones (C1, C2, C3 and C4) in the cooler by ambient air in cross flow up through the pellet bed. The outgoing process gas is recirculated to the kiln and to the grate giving an energy-efficient process. The cooler rotates with a speed which is determined by the production level and design of the cooler. At the end of the cooler the pellets are discharged for screening and external transport to customers.

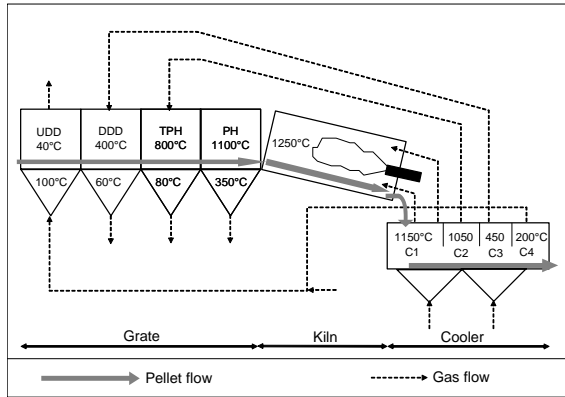


**Figure 1:** Flowsheet of Grate-Kiln process.

#### Introduction of research using CFD

Several research projects with application of CFD have been initiated by LKAB during 2005. MEFOS is a strategic partner for LKAB when it comes to metallurgical research and is therefore involved in the projects. Special knowledge from universities are used in different projects in order to reach project objectives. Table 1 gives an overview of ongoing projects and partners involved with projects applied on the pelletizing process.

Project	Focus / objectives	Partners
Grate-Kiln process	Pellet quality. Process design and improvements.	LKAB, MEFOS
Combustion modelling	Reduced emission of nitric oxides.	LKAB, KTH, MEFOS
Drying of iron ore pellets	Increased understanding of the fundamental mechanism for drying and heat transfer.	LKAB, LTU, MEFOS

**Table 1:** Pelletizing projects with CFD.

In the project “Combustion modelling” the third partner is KTH - Royal Institute of Technology, Division of Energy and Furnace Technology (KTH). The third partner in the

project “Drying of iron ore pellets” is Luleå University of Technology, Division of Fluid Mechanics (LTU).

In this paper a description of a pellet bed model and results are presented from the first project. Results from a parametric study is shown from the second project. Results from the project “Drying of iron ore pellets” is presented in a separate paper (Ljung and Lundström, 2006).

#### MODEL DESCRIPTION

##### General

The commercial code Fluent has been chosen as the platform for the calculation of flow and energy in the gas phase. User-defined subroutines have been developed in order to account for the implementation of porosity in the packed bed with momentum loss, gas-solid heat transfer, heat conduction within a pellet, heat conduction in the bed and radiation between the pellet surfaces in the bed.

##### Boundary conditions and calculation domain

Figure 2 shows a schematic figure of the annular cooler.

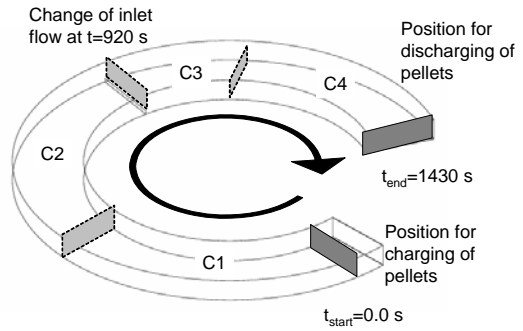


**Figure 2:** Simulation of a 2D bed moving in an annular cooler.

Pellets are charged into the cooler and discharged after three quarters of a full revolution. The cooler with the pellet bed rotates in a clockwise direction giving a total residence time of 1430 s. A production level of 540 tonnes per hour is simulated. The cooling process is simulated by movement of a 2D section with time. In this example, 1D, the bed height, is sufficient but a 2D structure has been prepared for future studies of different bed geometries and variations of bed porosities. A time step of 0.002 s is used.

Cooling air at a temperature of 273K enters from the bottom and leaves the domain at an atmospheric pressure, see Figure 3. In total 1560 cells are used for the domain and 546 are used for the bed. The total amount of cooling air is 1.5 kg per kilo pellet distributed over two time periods, 0-920 and 920-1430 s giving inlet velocities of 1.15 and 1.64 m/s.

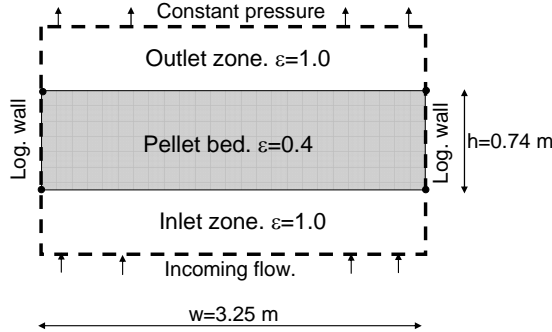


**Figure 3:** Calculation domain

### Model equations

Conservation equations in the transient form for mass, momentum and heat are set up and solved. The standard k-ε model has been used for the description of turbulence. No-slip conditions with standard logarithmic wall functions are used at the walls.

A source term has been included in the momentum equation to represent the pressure loss through the bed. The pressure loss in a bed per unit length has been described using a modified version of the Ergun equation (Ergun, 1952),

$$\frac{\Delta P}{\Delta x_i} = 180 \mu \frac{(1-\varepsilon)^2 U_i^2}{\varepsilon^3 (\phi d_p)^2} + 1.75 \rho \frac{(1-\varepsilon) U_i^2}{\varepsilon^3 (\phi d_p)} \quad (1)$$

Small scale experiments with low flow rates have given a slight higher constant compared to the original equation (180 vs. 150). The shape factor of the pellet,  $\phi$ , has been assumed to unity and an average pellet diameter,  $d_p$ , of 0.012 m has been used in the calculations.

The heat transfer between the process gas and the surface of the pellets is described by convection according to,

$$\Delta Q_{conv} = A_p \alpha_b (T_{surf} - T_{gas}) \Delta t \quad (2)$$

The heat transfer coefficient in a pellet bed is a function of the Nusselt number, the conductivity of the process gas and bed properties. An empirical relationship describing the Nusselt number as a function of the flow and bed properties has been used (Meyer, 1980),

$$\alpha_b = Nu \frac{\lambda_{gas}}{d_p} \frac{1-\varepsilon}{\varepsilon} \quad (3)$$

$$Nu = 2 \frac{\varepsilon}{1-\varepsilon} + Re_b^{0.5} + 0.005 Re_b \quad (4)$$

In the bed the energy could be transferred by conduction through the contact point between individual pellets. For a 2D quad mesh the conduction has been described according to,

$$\Delta Q_{cond_b} = \sum_{j=1}^4 \frac{A_{f,j}}{\sum A_{f,j}} A_p \frac{2}{3} \lambda_b \nabla T_j \Delta t \quad (5)$$

$A_{f,j}$  is the cell face area between cell 0 and cell j according to Figure 4.  $\nabla T_j$  is the thermal gradient between cell 0 and cell j.

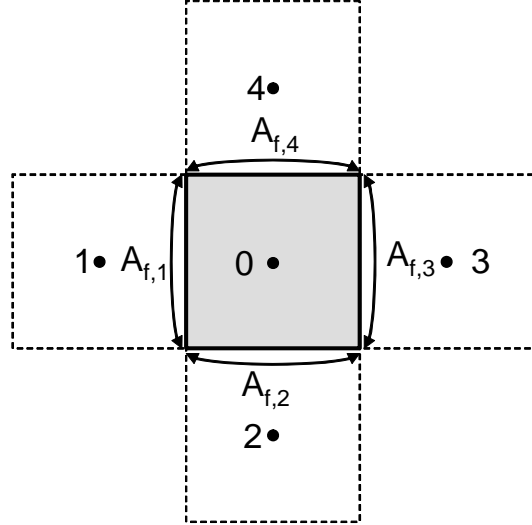


**Figure 4:** Cell face areas

The radiation heat transfer is simplified to black body radiation in an enclosed volume. Energy transferred by radiation from one cell to a neighbouring cell is estimated by,

$$\Delta Q_{rad} = \sum_{j=1}^4 \frac{A_{f,j}}{\sum A_{f,j}} A_p \frac{2}{3} \epsilon_{rad} \sigma (T_0^4 - (T_0 + \nabla T_j L_c)^4) \Delta t \quad (6)$$

$L_c$  is the average free radiation length, which has been estimated to one third of the pellet diameter.

### 1D single pellet model

Within a pellet the energy is transported by conduction. The pellet is divided into a number of radial layers, each with equal volume.

The energy transported from one layer k to another layer k+1, is described by,

$$\Delta Q_{cond_p} = 4 \lambda_p \frac{\pi}{1/r_k - 1/r_{k+1}} (T_{k+1} - T_k) \Delta t \quad (7)$$

### Properties

#### Gas

Air density and viscosity are functions of the temperature and pressure. The ideal gas law has been used for density and Sutherland's formula for description of viscosity. Tabulated values for different temperatures with linear interpolation have been used for thermal conductivity and heat capacity.

### Bed

The porosity in the bed varies depending of the size distribution of the pellets and the position in relation to the walls (Taylor et al., 1999; Guo et al., 2003). In this work constant bed porosity,  $\varepsilon$ , has been set to 0.4. The heat conduction in the bed,  $\lambda_b$ , has been set to 0.4  $\text{Wm}^{-1}\text{K}^{-1}$ .

### Pellet

A pellet density of  $3500 \text{ kg m}^{-3}$  has been set. Heat conduction within the pellet varies with the temperature and has been set according to Drugge (2002),

$$\lambda_p = 0.6 \cdot \left( 1 + \left( \frac{T}{900} \right)^2 \right) \quad (\text{Wm}^{-1}\text{K}^{-1})$$

The property of hematite has been used for the heat capacity of the pellet. The heat capacity varies with temperature according to Figure 5.

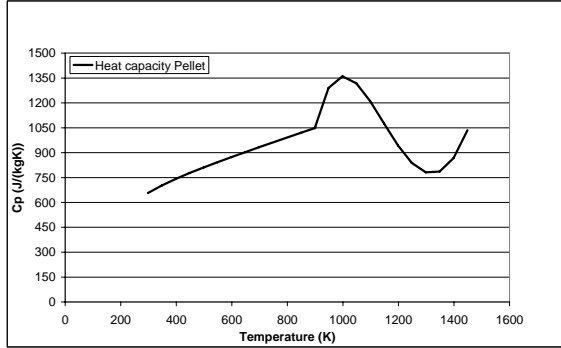


Figure 5: Heat capacity of the pellet.

## RESULTS

### Heat transfer model applied on annular cooler

The transient solver has been used for the prediction of the results. The solver is run to convergence on each time step. This implies that the iterative error is small, i. e. less than  $1\text{e}^{-3}$  for momentum and less than  $1\text{e}^{-6}$  for energy. Discretisation error has not yet been estimated.

Figure 6 shows the calculation domain with contours of the pellets surface temperature in Kelvin after 600 s of simulation. The lower half of the bed has decreased in temperature to a level of 300 to 750K. In the upper part of the bed temperatures are ranging from 750 to 1410K. The isotherms are not straight lines but wavy. This is due to the coupled calculation of flow, pressure and heat transfer. Unstable initial conditions and local variations in flow and pressure give local variations in pellet and gas temperatures.

Figure 7 demonstrates the temperature of the process gas which also shows wavy isotherms in the bed due to the coupled calculation. The pressure drop in the bed decreases when the bed cools down leading to a locally higher flow. This numerical phenomenon could be decreased by a finer mesh but could not be totally

avoided. The establishment of a uniform initial flow field is the key to avoid local variations.

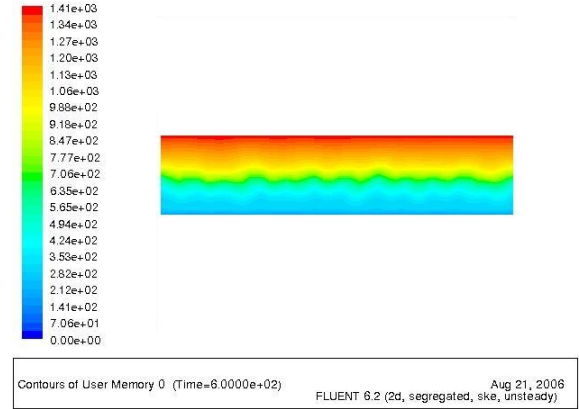


Figure 6: Temperature of the pellet surface after 600 s.

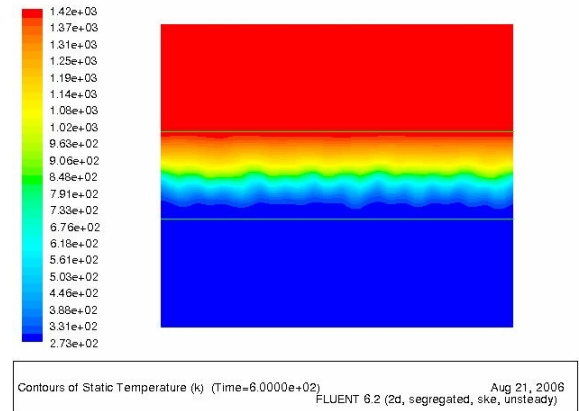


Figure 7: Temperature of the process gas after 600 s

Figure 8 shows the integrated outgoing temperature of the process gas together with the average temperature of the entire pellet bed. Measured outgoing temperatures from the four zones C1-C4 are also presented for comparison. It should be stressed that the simulation does not include any oxidation of remaining magnetite in the cooler. In this calculation a complete oxidation has been assumed as starting condition in the cooler. More than 50% of the energy in the Grate-Kiln process comes from the oxidation of magnetite to hematite.

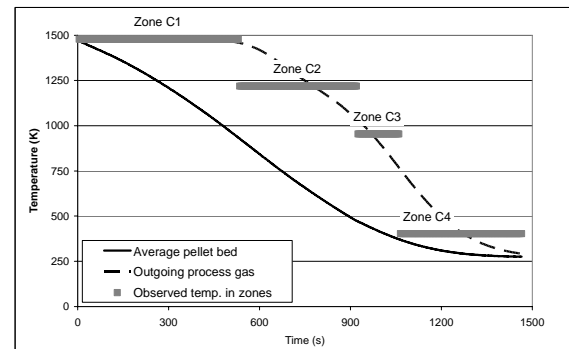
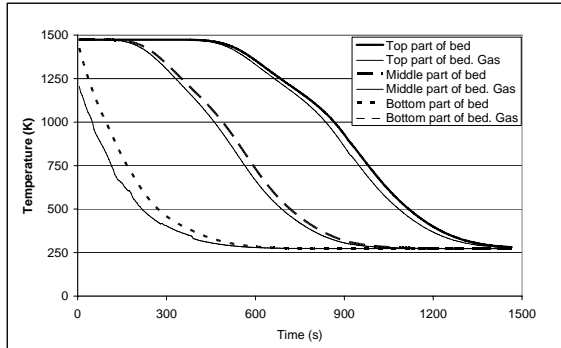


Figure 8: Calculation of pellet bed and process gas temperatures in annular cooler.

The oxidation degree of pellet coming from the kiln is varying and a realistic value is in the order of 95 %. A further oxidation of the remaining magnetite would increase the temperature approximately 20K. The calculated temperature of the process gas with or without oxidation agrees well with the measured values for cooling zones C1-C4.

Temperatures for three locations of the pellet surface temperature together with local gas temperatures are presented in Figure 9 (top, middle and bottom part of bed).



**Figure 9:** Pellet surface and gas temperatures at three different locations in annular cooler.

Average cooling rates of the pellet surface determined in the interval 500 to 1250K are -1.7, -2.0 and -3.2K/s for top, middle and bottom position. The fastest cooling rate is observed in the bottom part of the bed where the ambient cold gas is entering. The difference in temperature between pellet surface and gas is varying in time and position. A typical temperature difference is 50 to 100 K. The highest difference is 225K at the bottom of the bed and in the beginning of the simulation. Theoretically this value should be 1200K as a result of initial thermal conditions of the bed and incoming boundary conditions of the gas. An explanation to this discrepancy is in the procedure for extracting results from the calculation. Results have been extracted for every 5 seconds. The very first period with large differences in temperature is not included in Figure 9.

Temperature differences in a pellet and between gas and pellet surface are shown for the middle position in Figure 10. The maximum difference between gas and pellet surface is 72K after approximately 545 s. Maximum difference inside the pellet is 35K after 580 s.

It is obvious that the driving force for the heat transfer is varying with time. Temperature difference inside the pellet becomes more important with time due to a decreasing temperature and conduction in the pellet. This is also shown in Figure 11 where the heat transfer resistance is shown inside the pellet, i.e. conduction and at the pellet surface, i.e. convection.

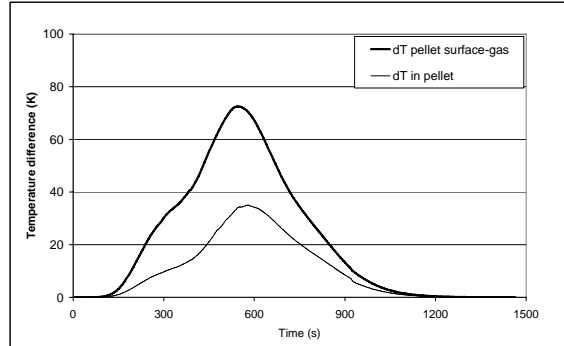


**Figure 10:** Temperature differences for middle position in bed.

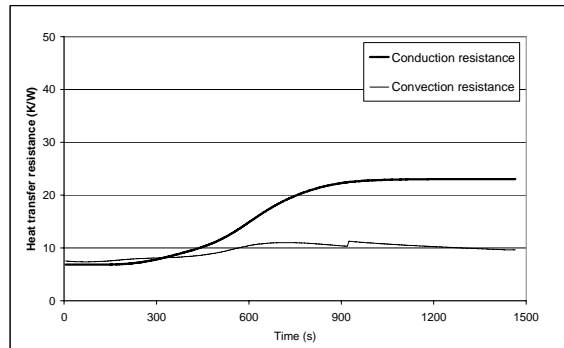


**Figure 11:** Heat transfer resistance in the middle position of the bed.

In the beginning of the simulation the two heat transfer modes are equal in magnitude. Inside the pellet the temperature is high giving a high thermal conduction. During the first 300 s the resistances are equal but from 300 s and on, the conductive resistance is higher than the convective resistance. This is due to a deceasing thermal conductivity in the pellet.

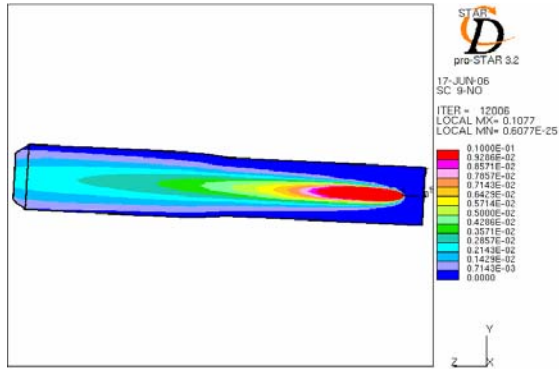
Heat transfer within a pellet will be further studied in combination with mass transfer. The rates of drying and oxidation are coupled with the heat transfer to the pellet and within the pellet. These coupled transport processes will be studied in the future.

#### Combustion modelling in kiln

This modelling has been performed by KTH in cooperation with LKAB and MEFOS (Yang et al. 2006). Combustion of coal and the formation of nitric oxides (NOX) have been studied. A Lagrangian/Eulerian concept has been used for the solid coal and the gas flows. Three mechanisms have been included for the generation of NOX; thermal, fuel and prompt NOX. The model has been set up in the software STAR-CD.

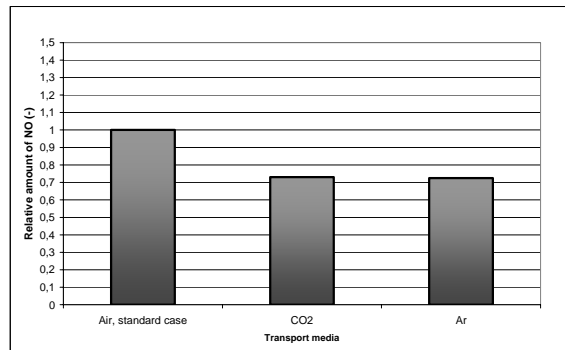
Parametric studies have been performed and the generation of NOX has been studied in relation to a standard production case.

Figure 12 shows the generation rate of NO of the standard case. NO is the most important compound of the nitric oxidises. The highest generation rate is in the flame region indicating the importance of combustion temperature.



**Figure 12:** Calculation of NO formation in kiln.

Figure 13 shows a result where the media of the pneumatic coal transportation system has been replaced by other gases than air.



**Figure 13:** Influence of the transport gas on amount of outgoing NOX from kiln.

According to the simulation a reduction of approximately 30 % could be achieved with CO<sub>2</sub> or Ar as media for the pneumatic transport of the coal into the burner.

## CONCLUSION AND FUTURE WORK

CFD has been introduced as a tool for process analysis at LKAB and applied on parts of the Grate-Kiln pelletizing process. Two examples of applications have been shown and in both cases the work is only at its beginning. The future work will consist of validation measurements parallel to model improvements. So far, validation measurements of pressure drop in packed beds have been done in laboratory scale and further measurements are planned for tuning of the developed mass and heat transfer model. Laboratory measurements of the drying and the oxidation process will be done in cooperation with LTU.

Validation measurements are also planned in the production scale for the purpose of the heat transfer process and for measurements of emissions. Sensors for nitric oxide have been installed and the first results are under investigation.

There are many possible model improvements which can be done. In general, the improvements must be done parallel with validation activities. Material transport properties, turbulence model and implementation of a local variation of porosity of the bed are areas of improvements.

However, the most important aspect of the model improvement is to increase the knowledge of the pelletizing process itself. The research programme which was initiated 2005 has created a common platform for LKAB and MEFOS in the area of pelletizing. Accurate modelling of a real process requires accurate data from the production plant. During the project work a number of questions have been raised which need further investigations in the plant. In this project the CFD work is truly applied and the future work will show how far it is possible to reach.

## REFERENCES

- DRUGGE R., (2002), "Model for oxidation and heat transfer in one pellet", *Internal report LKAB*.
- ERGUN S., (1952), "Fluid flow through packed columns", *Chemical Engineering Process*, **48** No. 2, 89-94.
- GUO, B., YU, A., WRIGHT, B., and ZULLI, P., (2003), "Comparison of several turbulence models applied to the simulation of gas flow in a packed bed", *Third International Conference on CFD in the Minerals and Process Industries*, CSIRO, Melbourne, Australia, December 10-12.
- LJUNG, Anna-Lena and LUNDSTRÖM, T.S. (2006), "Drying of iron ore pellets", *Fifth International Conference on CFD in the Minerals and Process Industries*, CSIRO, Melbourne, Australia, December 13-15.
- MEYER K., (1980), "Pelletizing of Iron Ores", Springer Verlag Düsseldorf, ISBN 3-514-00245-0.
- TAYLOR, K., SMITH, A.G., ROSS, S., and SMITH, M., (1999), "The prediction of pressure drop and flow distribution in packed bed filters", *Second International Conference on CFD in the Minerals and Process Industries*, CSIRO, Melbourne, Australia, December 6-8.
- YANG, W., KAKIETEK, S., and BLASIAK, W., (2006), "Research and project work in progress".